NATIONAL ADVISORY COMMITTEE FOR AERONAUTICS

TECHNICAL NOTE 2464

TWO AXIAL-SYMMETRY SOLUTIONS FOR INCOMPRESSIBLE FLOW THROUGH A CENTRIFUGAL COMPRESSOR WITH AND WITHOUT INDUCER VANES

By Gaylord O. Ellis, John D. Stanitz, and Leonard J. Sheldrake

Lewis Flight Propulsion Laboratory
Cleveland, Ohio

Washington
September 1951

NATIONAL ADVISORY COMMITTEE FOR AERONAUTICS

TECHNICAL NOTE 2464

TWO AXIAL-SYMMETRY SOLUTIONS FOR INCOMPRESSIBLE FLOW THROUGH A CENTRIFUGAL COMPRESSOR WITH AND WITHOUT INDUCER VANES

By Gaylord O. Ellis, John D. Stanitz, and

Leonard J. Sheldrake

SUMMARY

Solutions for axially symmetric flow through an impeller with and without inducer vanes were obtained by relaxation methods using an analysis developed herein. The fluid was considered inviscid and incompressible. The impeller selected was of arbitrary design except that the impeller blades were assumed to have zero thickness and to consist of radial elements. Plots of streamlines, lines of constant velocity, and lines of constant tangential blade force (related to the pressure difference between blade surfaces) are presented and discussed.

For impellers with thin, high-solidity blades, the effects of inducer vane curvature on the streamlines and on the axial and radial components of velocity were found to be small and were restricted to those regions in which the vanes were curved.

INTRODUCTION

Although trial-and-error methods of development may result in centrifugal compressors of acceptable efficiency, they can provide only design information based on geometric properties and not on fundamental aerodynamic principles. Without design information based on fundamental principles, the experience of previous developments cannot easily be applied to the design of new compressors with different geometry or operating requirements, nor in general can essential features of a good design be separated from those having little effect on performance. The flow must therefore be experimentally and theoretically investigated in order that fundamental laws of design may be formulated which can be combined with designing skill to produce consistently good compressors.

For a given set of operating conditions, the flow in a centrifugal compressor depends on the compressibility and viscosity of the fluid and on the three-dimensional geometry of the compressor. In order that the flow may be analyzed without prohibitive effort, the fluid is usually assumed to be inviscid, and for some investigations the effects of compressibility are neglected. Also, in most analyses, variations in the flow are limited to two dimensions lying either on a plane containing the axis of the impeller (designated the meridional plane) or on a surface of revolution (designated the blade-to-blade plane) generated by rotating some characteristic line in the meridional plane (for example, the mean line between the hub and the shroud) about the axis of the impeller.

Several methods of analyzing the flow on the blade-to-blade plane have been developed (references 1 through 3, for example) and used to obtain detailed pictures of the flow on this plane. In particular, the method developed in references 1 and 2 has been used to investigate the effects on the flow of several blade-design and operating parameters (references 4 and 5).

Methods of analysis for flow on the meridional plane are developed in references 6 and 7. A similar method was used in a theoretical investigation made at the NACA Lewis laboratory to determine the general trend of some effects of blade curvature on the flow in the meridional plane of impellers in conventional centrifugal compressors, and the results are reported herein. The investigation consisted of two solutions for incompressible, frictionless flow through a typical impeller with straight impeller blades and with straight or curved inducer vanes. The general trends indicated by the results of these two examples are believed typical and, for the most part, applicable to other centrifugal-type compressors with either compressible or incompressible fluids.

METHOD OF ANALYSIS

Assumptions. - In this investigation, solutions were obtained for the flow of an incompressible, nonviscous fluid through the impeller of a centrifugal compressor with zero whirl upstream of the impeller. The flow was assumed to be axially symmetric (infinite number of compressor blades) with the velocities directed along the blade surfaces. In reference 8, Ruden shows that the assumption of an infinite number of blades gives a reasonable picture of the mean flow between blades with finite spacing, provided that the blade spacing is small enough.

The compressor geometry was chosen arbitrarily except that the blades were required to have no thickness and to consist of radial blade elements.

Coordinate system. - The cylindrical coordinates R, θ, and Z shown in figure 1 are convenient to use in theoretical studies of the flow in impellers of centrifugal compressors. These coordinates are dimensionless, as the linear coordinates R and Z have been divided by the impeller tip radius r_T (so that R equals 1.0 at the impeller tip, for example). The coordinate system rotates about the Z-axis with the angular velocity ω of the impeller.

Velocity components. - The velocity Q relative to the rotating coordinate system has components Q_R, Q_θ, and Q_Z in the R-, θ-, and Z-directions, respectively (fig. 1). These velocities are dimensionless as a result of division by the tip speed of the impeller ωr_T.

Ratios of the various velocity components are used to indicate the direction of a tangent to a streamline by defining the angles α, β, and ϵ (fig. 1), where

$$\tan \alpha = \frac{Q_R}{Q_Z} \tag{1a}$$

$$\tan \beta = \frac{Q_\theta}{\sqrt{Q_R^2 + Q_Z^2}} = \frac{Q_\theta}{Q_M} \tag{1b}$$

$$\tan \epsilon = \frac{Q_\theta}{Q_Z} \tag{1c}$$

(The symbols used herein are defined in appendix A.)

Differential equation. - With the effect of blade thickness neglected, the axially symmetric flow of a nonviscous, incompressible fluid through a centrifugal compressor having radial blade elements but of otherwise arbitrary geometry is given by equation (B8) (see appendix B):

$$(1 + \tan^2 \epsilon) \frac{\partial^2 \psi}{\partial R^2} + \frac{\partial^2 \psi}{\partial Z^2} + \frac{\tan^2 \epsilon - 1}{R} \frac{\partial \psi}{\partial R} + 2R \tan \epsilon = 0 \tag{B8}$$

where ψ is the stream function defined by

$$\left.\begin{aligned} \frac{\partial \psi}{\partial R} &= RQ_Z \\ \frac{\partial \psi}{\partial Z} &= -RQ_R \end{aligned}\right\} \tag{B7}$$

Numerical procedure. - Equation (B8) is solved by relaxation methods (references 9 and 10) to satisfy the specified compressor geometry and operating conditions. The relaxation process was performed on a grid of equally spaced points with seven grid spaces from hub to shroud upstream of the impeller. The finite-difference expressions were based on a second-degree polynomial and the residuals were reduced to give five-figure accuracy for the value of ψ at each grid point. Boundary conditions along the hub and shroud are satisfied by making ψ equal to a constant along each of these surfaces. Far upstream and downstream of the impeller, the flow is assumed uniform and the moment of momentum is assumed constant in all directions. It can be shown by differentiating the expression for constant moment of momentum and substituting into it the equations (B7) that

$$\tan^2 \epsilon \frac{\partial^2 \psi}{\partial R^2} + \frac{\tan^2 \epsilon}{R} \frac{\partial \psi}{\partial R} + 2R \tan \epsilon = 0 \tag{2}$$

so that equation (B8) becomes

$$\frac{\partial^2 \psi}{\partial R^2} + \frac{\partial^2 \psi}{\partial Z^2} - \frac{1}{R} \frac{\partial \psi}{\partial R} = 0 \tag{3}$$

Equation (3) was used to determine the distribution of ψ upstream and downstream of the impeller where the moment of momentum was constant.

NUMERICAL EXAMPLES

Description of impeller. - Axial-symmetry solutions were obtained for two examples of flow through an impeller with straight blades of zero thickness. Dimensions of the impeller profile in the meridional plane (hub-shroud contour) are indicated in figure 2.

For example I, the inducer vanes (region B, fig. 2) were assumed to be located immediately upstream of the impeller (region C) and are described by

$$\tan \epsilon = \frac{R d\theta}{dZ} = 2.917 \, R \, \frac{Z - 0.2333}{0.2333} \tag{4}$$

For example II, the inducer vanes were removed and the straight impeller blades extended indefinitely upstream parallel to the axis of the compressor. Thus for example II, $\tan \epsilon = 0$ everywhere up to the impeller tip.

A vaneless diffuser was assumed in both examples.

Conditions of solution. - Both examples were solved for the same ratio of impeller tip speed to volume flow rate, corresponding to a value of Q_Z equal to 0.3429 upstream of the impeller.

Two solutions were obtained for example I (impeller with inducer vanes) using different entrance conditions at the inducer inlet. For the first solution (example IA), a fictitious force field was assumed to act upstream of the inducer to add whirl at each radius so that the air entered the blades everywhere with zero angle of attack. This condition was satisfied numerically by the assumption that the vanes were continued upstream from the inducer inlet at a constant angle ϵ for each radius equal to the angle ϵ at the inducer inlet, where

$$\tan \epsilon = \frac{R d\theta}{dZ} = - 2.917 R \qquad (5)$$

until the vanes were completely unloaded.

For the second solution (example IB), the whirl of the fluid everywhere upstream of the inducer was assumed zero, so that just upstream of the blade entrance the tangential velocity Q_θ of the air relative to the rotating impeller was equal to minus the tangential velocity of the impeller, which is equal to R. Therefore, from equation (1c) with the subscript 1 indicating a point just upstream of the blade,

$$\tan \epsilon_1 = \frac{Q_\theta}{Q_Z} = - \frac{R}{Q_Z}$$

Just inside the bladed region the air is required, by the condition of axial symmetry, to be perfectly guided by the blade so that

$$\tan \epsilon_2 = \frac{R d\theta}{dZ}$$

where the subscript 2 indicates a point just inside the blade. The angle of attack will then be zero when

$$\tan \epsilon_1 = \tan \epsilon_2$$

or when

$$\frac{-1}{Q_Z} = \frac{d\theta}{dZ}$$

which is equal to a constant for radial blade elements. It will be shown later, however, that Q_Z is not a constant across the passage at the inlet, and therefore the angle of attack cannot be equal to zero everywhere.

The first solution (IA) has the advantage of a continuous axial-symmetry solution but requires that hypothetical blade forces act upstream of the inducer. The second solution (IB) has the advantage of more nearly representing the flow conditions upstream of the inducer but has the disadvantage of a sudden change in flow direction at the inducer inlet. This change is physically incorrect and results in a discontinuous axial-symmetry solution.

RESULTS AND DISCUSSION

Streamlines. - Streamlines for solutions to the two axial-symmetry examples are shown in figures 3 and 4. The streamlines are designated by a stream-function ratio such that the value of the streamline indicates the percentage of flow through the compressor between the streamline and the impeller hub. At a given radius the streamline spacing is indicative of the meridional velocity Q_M, with close spacing indicating high velocities and wide spacing indicating low velocities.

The streamlines for example IA (force field assumed to be acting upstream of the inlet) are shown in figure 3(a). In figure 3(b), the streamlines for example IB (zero whirl upstream of the inlet) are compared with the streamlines obtained for example IA. Examination of the two solutions shows that for the stream-function distribution, the mathematical treatment of inlet condition is not of great importance; either method gives approximately the same streamline picture.

In figure 4, the streamlines for example IA are compared with the streamlines for example II (the impeller with inducer vanes removed and straight impeller blades extended indefinitely upstream). The stream-function distribution is very nearly the same everywhere, indicating that, at least for thin blades and incompressible flow, blade curvature about the axis of the compressor (associated with the angle ϵ) has only a small effect on the stream-function distribution for axial-symmetry solutions.

It is interesting to note that for example II, in which $\tan \epsilon$ equals zero everywhere, the differential equation for the distribution of ψ is given by equation (3), which is identical to the differential equation for the distribution of ψ in axially symmetric flow with no impeller blades (reference 11). Thus for incompressible flow, the stream-function distribution in the meridional plane is the same, with or without thin straight blades, and approximately the same if the blades are curved about the axis of the compressor.

Lines of constant relative velocity. - In figure 5(a), lines of constant relative velocity Q are plotted for example IA (impeller with inducer vanes located immediately upstream of the straight impeller blades and a force field assumed to be acting upstream of the inlet). In section A ahead of the inducer vanes, the velocity accelerates along the shroud and decelerates along the hub because of subsequent curvature in the hub-shroud contour, as when approaching any duct elbow. In the inducer (section B), the relative velocity decreases along all streamlines as a result of the turning in the inducer vanes, which increases the relative flow area between blades. In the impeller (section A), the velocity accelerates along the hub but remains almost constant along the shroud. This behavior is the result of two effects: (1) a 50-percent decrease in the annulus cross-sectional area of the impeller, which tends to accelerate the flow along the hub and shroud; and (2) a rather sharp elbow profile (fig. 2), which tends to accelerate the flow along the hub and to decelerate the flow along the shroud following the points of maximum curvature along the hub and shroud, respectively. These two effects add along the hub, causing the flow to accelerate, but subtract along the shroud, causing the velocity to remain almost constant. The relative velocity rapidly becomes uniform across the passage in the vaneless diffuser and increases indefinitely as the absolute velocity approaches zero with increasing radius, as required by constant moment of momentum.

In figure 5(b), lines of constant velocity for example IB (whirl upstream of inducer equal to zero) are compared with those of example IA (force field assumed to be acting upstream of inlet). The discontinuity in the velocities for example IB is caused by the sudden change in tangential velocity of the air as it meets the blade at an angle of attack. This angle of attack is discussed in the section "Angle of attack."

In general, the velocity plots for examples IA and IB are similar and, as for the stream-function distribution, the mathematical treatment of inlet conditions has little effect (in the impeller) for small angles of attack.

In figure 6, lines of constant Q are plotted for example II (impeller with inducer vanes removed and straight impeller blades extended indefinitely upstream). For this example, the value of Q far upstream of the impeller elbow is equal to 0.3429, which is the specified value of Q_z given previously. A comparison of figures 5 and 6 shows that, although the velocities are quite different in those regions where the blade geometry is different (sections A and B, fig. 2), the velocities are very much the same in regions where the blade geometry is the same (section C, fig. 2). Therefore, for incompressible, axially symmetric flow in impellers with thin blades, the effect of vane curvature on velocity distribution is limited to those regions in which the curvature occurs if the flow is assumed everywhere tangent to the mean blade surface.

If the velocities of example II ($\tan \epsilon$ equal zero) are modified by adding a tangential component of velocity Q_θ equal to $Q_Z \tan \epsilon$ (where the $\tan \epsilon$ distribution is the same as in example I), the resultant velocities are a good approximation for the velocities of example I. The velocities obtained by modifying the solution for example II are compared with the velocities obtained from the solution for example IA in figure 7. From the results shown in this figure, the velocity Q_M in the meridional plane, the resultant of Q_R and Q_Z, is concluded to be essentially independent of the blade shape and determined primarily by the hub-shroud contour. These results are in agreement with and could be expected from the fact that the stream-function distribution was approximately the same for both solutions. If the effects of compressibility and blade-thickness variation are not too great, hub-shroud contours can therefore be designed for distributions of Q_R and Q_Z that are independent of the blade shape developed later for the impeller.

Lines of constant tangential blade force. - In appendix C, rational solutions for axially symmetric flow through impellers of centrifugal compressors are shown to require a distributed blade force, the tangential component of which is related to the pressure difference between the surfaces of blades with finite spacing. This tangential component multiplied by a coefficient $g/\omega^2 r_T$ to correct for the rotational speed of the impeller is given in appendix C by

$$\left(\frac{g}{\omega^2 r_T}\right) F_\theta = \frac{2Q}{R}\left(R + Q_\theta\right)\frac{dR}{dL} + Q^2 R\left(\frac{1}{Q}\frac{dQ}{dL}\frac{d\theta}{dL} + \frac{d^2\theta}{dL^2}\right) \qquad (C3)$$

where

L distance measured along a streamline (not necessarily confined to meridional plane) divided by r_T

F distributed blade force per unit weight of fluid

The first term on the right side of equation (C3) represents the blade force due to radial displacement of the flow (Coriolis force), and the last term represents the blade force due to the tangential acceleration of the fluid caused by the blade turning. Plots of the tangential blade force for the three examples appear in figures 8 and 9.

In figure 8(a) appear lines of constant $\left(\frac{g}{\omega^2 r_T}\right) F_\theta$ for example IA (impeller with inducer vanes located immediately upstream of straight impeller blades).

For this example, a fictitious force field was assumed to act upstream of the inlet to add whirl (moment of momentum) to the flow so that the fluid entered the blades with zero angle of attack. It will be shown in the section "Angle of attack" that the air tends to approach the inducer vanes with an angle of attack that is positive near the hub but negative at the shroud. Thus the force field must be positive at the hub and negative at the shroud (positive force acts in the direction of rotation) as shown in figure 8(a).

In the inducer (section B), the distribution of tangential blade force F_θ results from both the blade turning and radial displacement terms in equation (C3). In the impeller (section C) where $\tan \epsilon$ equals zero so that the blade turning term in equation (C3) is zero, the distribution of F_θ results from the radial displacement term in equation (C3).

The discontinuities in F_θ at the entrance to the inducer vanes, at the line where the curved inducer vanes meet the straight blades of the impeller, and at the impeller tip result from the fact that the flow is everywhere directed tangent to the blade surface. (These discontinuities will be discussed.)

For example IB, the moment of momentum remains zero up to the impeller inlet so that no forces exist in the flow, as shown by figure 8(b). Comparison of figures 8(a) and 8(b) shows that except near the inlet the tangential blade forces are the same for example IA and IB, and, as for the streamlines and velocity distribution, the mathematical treatment of the inlet conditions has little effect on the solution provided that the angles of attack are not large.

Lines of constant $\left(\frac{g}{\omega^2 r_T}\right)F_\theta$ are plotted in figure 9 for example II (impeller with inducer removed and straight impeller blades extended indefinitely upstream). Because $\tan \epsilon$ equals zero everywhere, the blade forces result only from the radial displacement term of equation (C3). Comparison of figures 8 and 9 indicates that the distribution of F_θ is essentially the same in the impeller (section C) for impellers with or without inducer vanes. For incompressible, axially symmetric flow in impellers with thin blades, the effect of vane curvature is therefore limited to those regions in which the curvature occurs if the flow is assumed everywhere tangent to the mean blade surface.

The discontinuities in the distribution of F_θ in figures 8 and 9 can be shown by equation (C3) to result from discontinuity in $d^2\theta/dL^2$ along the blade surface. From figure 1,

$$\frac{d\theta}{dL} = \frac{1}{R} \tan \epsilon \cos \alpha \cos \beta$$

and $d^2\theta/dL^2$ is therefore, in general, discontinuous if $d(\tan \epsilon)/dL$, $d(\cos \alpha)/dL$, or $d(\cos \beta)/dL$ is discontinuous.

For the solutions obtained herein, the axially symmetric flow in the impeller is assumed to be directed tangent to the blade surface described by equations (4) and (5). From these equations, $d(\tan \epsilon)/dZ$ and therefore $d(\tan \epsilon)/dL$ are discontinuous at the inlet, and along a line that separates the straight impeller vanes from the curved inducer vanes. In the diffuser, the flow is assumed to be tangent to the straight impeller blades at the tip, but curved in such a manner as to maintain a constant moment of momentum. Thus as the tip of the impeller is approached along a streamline from inside the impeller, $d(\cos \alpha)/dR$ is equal to zero, but when the tip is approached from some position outside the impeller, $d(\cos \alpha)/dR$ approaches some finite value. Thus $d(\cos \alpha)/dR$ and therefore, in general, $d(\cos \alpha)/dL$ are discontinuous at the tip.

For axially symmetric flow that is everywhere tangent to the mean blade surface in example I, the tangential component of distributed blade force is therefore discontinuous at the inlet, at a line separating the curved inducer vanes from the straight blades of the impeller, and at the impeller tip, as shown in figure 8.

Axially symmetric flow not directed tangent to a mean blade surface. - A more realistic picture of the mean flow through blades having finite spacing might be obtained if the axially symmetric flow were assumed to lie on a surface that deviates from the mean blade surface in a manner similar to the deviation of the mean streamline on a surface of revolution. Such a surface would have no discontinuities in $d^2\theta/dL^2$; therefore the blade force would be continuous.

As was concluded in the discussion of the velocities, the blade curvature affects the flow only in those regions where the curvature occurs when the flow is everywhere directed tangent to the blade surface. If, however, the flow is assumed to be on a surface that deviates from the mean blade surface, the deviation may persist beyond the region of the blade curvature and cause variation in the axially symmetric flow. Thus an investigation of the effect of blade curvature on the flow in the meridional plane is not complete without some investigation of the mean flow on blade-to-blade planes as given by the mean streamline of this flow.

The deviation of the mean streamline of the flow on a blade-to-blade plane from the mean blade surface depends on:

(1) The blade spacing

(2) The angle through which the fluid is turned

(3) The rate of turning

The flow between inducer vanes in which the velocities have no radial component is shown in figure 10. The three examples give a range of turning angle $\Delta\beta$ from 0° to 90° at an infinite rate of turning. The solution for zero turning is obvious. The solution for 45° turning was obtained by relaxation methods, and the solution for 90° turning was obtained from the imaginary part of the complex expression

$$w = \ln \sin (Z + iR\theta)$$

For 45° turning, appreciable deviation (as indicated by shaded area) extends only about one-half channel width downstream and at 90°, one channel width downstream. Thus, for a given rate of turning, it appears that the mean streamline deviates from the mean blade line a distance downstream from the region of turning which is directly proportional to the amount of turning. In figure 2, the dashed line DE shows the distance downstream the mean flow surface would deviate from the mean blade surface under this assumption if all the turning (infinite rate of turning) occurred along the line FG that divides the inducer section B from the impeller section C. This distance is not great, and in the actual case with finite rates of turning for the curvature in the inducer section, the deviation should not extend so far downstream.

It is therefore concluded that for incompressible, nonviscous flow through impellers with thin high-solidity blades, the effect of blade curvature, including the effect of deviation of the mean flow from the mean blade surface, does not extend far beyond the region of the blade curvature.

Effects of compressibility. - As fluid passes through a centrifugal impeller, there is an increase in density, which requires a decrease in velocity. Along the shroud, for example, where the velocity was almost constant for an incompressible fluid (see fig. 3), the velocity in a compressible fluid would be expected to decelerate with attending increases in boundary layer and losses in efficiency. Thus compressors using compressible fluids are usually less efficient than pumps using incompressible fluids.

Because for compressible solutions disturbances are propagated with a finite speed of sound compared with an infinite speed for incompressible solutions, conditions upstream of a given point would be expected

to have, at most, no more effect on flow conditions at the point for a compressible fluid than for an incompressible one. The general tendencies indicated by the results of the examples in this report are therefore believed to be applicable to impellers with compressible flow.

Effects of blade taper. - Blade taper at the inlet would shift the streamlines from the hub toward the shroud for some distance upstream of the inducer inlet. This shift results in an increase in velocity along the shroud and a decrease along the hub, which is an effect similar to that of curvature in the hub-shroud contour (see section entitled "Lines of constant relative velocity").

2241

Angle of attack. - The discontinuity in the velocity at the entrance to the inducer vanes for example IB (shown by dashed lines in fig. 5(b)) is caused by a sudden change in the tangential velocity of the air as it meets the blade at a finite angle of attack. As indicated in the section "Conditions of solution," this angle of attack is due to the increased velocity on the shroud (fig. 11), which causes the air to enter the blade at an angle less than the blade inlet angle (negative angle of attack), and the decreased velocity on the hub (fig. 11), which causes the air to enter the blade at an angle greater than the blade inlet angle (positive angle of attack), with the blade entrance angle assumed designed for zero angle of attack with uniform entrance conditions. The variations in axial velocity across the passage, shown in figure 11, were caused by the curvature in the hub-shroud contour inside the impeller region. Blade taper may have a similar effect, as was shown in the previous section. In addition, the passage leading into the impeller may have an important effect upon the axial-velocity profile at the inlet. The geometric factors causing variation in axial velocity across the passage must always result in a variation of the angle of attack across the passage for blades with radial elements and a straight radial leading edge.

SUMMARY OF RESULTS AND CONCLUSIONS

For incompressible, frictionless flow which is axially symmetric, the following results and conclusions are indicated by the examples of this report:

1. If the mean flow surface is assumed to coincide with the mean blade surface, the effect of the blade curvature is not extended far beyond the region of the curvature.

2. The effect of blade curvature on the flow beyond the region of the curvature is determined by the deviation of the mean flow surface from the mean blade surface. For high-solidity blades, such as exist in centrifugal impellers, this deviation is small and is limited to the immediate vicinity of the region in which the blades are curved.

3. The stream-function distribution and the component of velocity lying in the meridional plane (resultant of the radial and axial components of velocity) were determined primarily by the hub-shroud contour, for they are similar with and without blades or for blades with radically different curvatures. Therefore, if the effects of compressibility and blade-thickness variation are not too great, hub-shroud contours can be designed for distributions of axial and radial velocities that are independent of the blade shape developed later for the impeller.

4. Large discontinuities in the computed blade forces can be avoided if the flow is assumed to be on a mean flow surface containing the mean streamlines of blade-to-blade solutions.

5. For blades having radial elements and a straight radial leading edge, the angle of attack at the inducer inlet varies from hub to shroud because of the variation in axial velocity across the passage.

6. Variations in axial velocity at the inlet resulted from curvature in the hub-shroud contour of the impeller. The blade taper and the hub-shroud contour of the passage upstream of the inlet may also result in similar variations.

Lewis Flight Propulsion Laboratory,
National Advisory Committee for Aeronautics,
Cleveland, Ohio, June 7, 1951.

APPENDIX A

SYMBOLS

The following symbols are used in this report:

F	distributed blade force per unit weight of fluid
g	acceleration due to gravity
L	distance measured along streamline (not necessarily in meridional plane) divided by impeller tip radius r_T
P	pressure ratio, p/p_o
p	static (stream) pressure
Q	dimensionless velocity relative to impeller (expressed as ratio of ωr_T)
q	velocity relative to impeller
R,Z,θ	dimensionless cylindrical coordinates relative to impeller (R and Z expressed as ratios of r_T; θ positive counterclockwise when viewed in minus Z-direction)
r,z,θ	cylindrical coordinates relative to impeller
α	angle whose tangent is Q_R/Q_Z
β	angle whose tangent is $\dfrac{Q_\theta}{\sqrt{Q_R^2+Q_Z^2}}$
$\Delta\beta$	turning angle in inducer
ϵ	angle whose tangent is Q_θ/Q_Z
ρ	static (stream) weight density
ψ	stream function, defined by equation (B7)
ω	angular velocity of impeller

Subscripts:

M	component lying in meridional plane

o	stagnation condition upstream of impeller
R,Z,θ or r,z,θ	components in R-, Z-, θ- or r-, z-, θ-direction, respectively (positive in direction of increasing R, Z, θ)
T	impeller tip

APPENDIX B

METHOD OF ANALYSIS FOR INCOMPRESSIBLE FLOW WITH AXIAL SYMMETRY IN COMPRESSORS AND TURBINES WITH RADIAL BLADE ELEMENTS

The radial component of Lorenz's equation of motion for steady, axially symmetric flow is given by (reference 12)

$$q_r \frac{\partial q_r}{\partial r} + q_z \frac{\partial q_r}{\partial z} - \frac{(q_\theta + \omega r)^2}{r} + \frac{g}{\rho} \frac{\partial p}{\partial r} = 0$$

if the blade elements are radial ($F_R = 0$). In terms of the relative velocity and coordinate ratios defined in appendix A, this equation becomes

$$Q_R \frac{\partial Q_R}{\partial R} + Q_Z \frac{\partial Q_R}{\partial Z} - \frac{(Q_\theta + R)^2}{R} + \frac{g\, p_o}{\rho(\omega r_T)^2} \frac{\partial P}{\partial R} = 0 \qquad \text{(B1)}$$

In terms of the same relative velocities and coordinate ratios, Bernoulli's equation for steady, incompressible flow relative to a coordinate system rotating with the angular velocity ω becomes (reference 13):

$$\frac{Q_R^2}{2} + \frac{Q_Z^2}{2} + \frac{Q_\theta^2}{2} - \frac{R^2}{2} + \frac{g\, p_o}{\rho(\omega r_T)^2} P = \text{constant} \qquad \text{(B2)}$$

Differentiating equation (B2) with respect to R and combining with equation (B1) to eliminate the terms involving P give

$$Q_Z\left(\frac{\partial Q_Z}{\partial R} - \frac{\partial Q_R}{\partial Z}\right) + Q_\theta \frac{\partial Q_\theta}{\partial R} + \frac{Q_\theta^2}{R} + 2\, Q_\theta = 0 \qquad \text{(B3)}$$

From equation (1c),

$$Q_\theta = Q_Z \tan \epsilon$$

so that

$$\frac{\partial Q_\theta}{\partial R} = \tan \epsilon \frac{\partial Q_Z}{\partial R} + Q_Z \frac{\partial(\tan \epsilon)}{\partial R} \tag{B4}$$

For radial blade elements,

$$\frac{\tan \epsilon}{R} = f(Z)$$

so that

$$\frac{1}{R} \frac{\partial(\tan \epsilon)}{\partial R} - \frac{\tan \epsilon}{R^2} = 0$$

or

$$\frac{\partial(\tan \epsilon)}{\partial R} = \frac{\tan \epsilon}{R} \tag{B5}$$

Combining equations (1c), (B3), (B4), and (B5) gives

$$(1 + \tan^2 \epsilon) \frac{\partial Q_Z}{\partial R} - \frac{\partial Q_R}{\partial_Z} + 2 \tan^2 \epsilon \frac{Q_Z}{R} + 2 \tan \epsilon = 0 \tag{B6}$$

For axially symmetric flow of an incompressible fluid through a compressor or turbine having blades of zero thickness, a stream function satisfies the continuity equation if defined as

$$\left.\begin{aligned} \frac{\partial \psi}{\partial R} &= R\, Q_Z \\ \frac{\partial \psi}{\partial Z} &= -R\, Q_R \end{aligned}\right\} \tag{B7}$$

Equations (B7) and (B6) are combined to give

$$(1 + \tan^2 \epsilon) \frac{\partial^2 \psi}{\partial R^2} + \frac{\partial^2 \psi}{\partial Z^2} + \frac{\tan^2 \epsilon - 1}{R} \frac{\partial \psi}{\partial R} + 2 \tan \epsilon = 0 \tag{B8}$$

Equation (B8) is solved by relaxation methods to obtain the solutions presented in figures 3 through 9.

APPENDIX C

DISTRIBUTED BLADE FORCE

In the absence of body forces resulting from some arbitrary force field, the moment of momentum of fluid particles in axially symmetric flow must remain constant because the pressure is independent of θ. Conversely, if the moment of momentum is not a constant in axially symmetric flow, a body force F must be assumed to exist, the tangential component of which is proportional to the rate of change in the moment of momentum. In impellers with a finite number of blades, the change in moment of momentum results from pressure differences on the two surfaces of each blade. The blade forces resulting from these pressure differences approach zero as the number of blades approaches infinity, but the weight of fluid contained between the blades also approaches zero, and the ratio of blade force to weight of fluid approaches a value which is the body force or "distributed blade force" of axially symmetric flow.

The tangential component of Lorenz's equation of motion for steady, axially symmetric flow is given by (reference 12)

$$g F_\theta = q_r \frac{\partial q_\theta}{\partial r} + q_z \frac{\partial q_\theta}{\partial z} + 2\omega q_r + \frac{q_r q_\theta}{r}$$

In terms of the relative velocity and coordinate ratios defined in appendix A, this equation becomes

$$\left(\frac{g}{\omega^2 r_T}\right) F_\theta = Q_R \frac{\partial Q_\theta}{\partial R} + Q_Z \frac{\partial Q_\theta}{\partial Z} + 2 Q_R + \frac{Q_R Q_\theta}{R} \qquad (C1)$$

But from figure 1,

$$Q_R = Q \frac{dR}{dL}$$

$$\frac{Q_\theta}{R} = Q \frac{d\theta}{dL}$$

$$Q_Z = Q \frac{dZ}{dL}$$

so that equation (C1) becomes

$$\left(\frac{g}{\omega^2 r_T}\right)F_\theta = Q\frac{\partial Q_\theta}{\partial R}\frac{dR}{dL} + Q\frac{\partial Q_\theta}{\partial Z}\frac{dZ}{dL} + 2Q\frac{dR}{dL} + \frac{Q_\theta}{R}Q\frac{dR}{dL}$$

$$= Q\frac{dQ_\theta}{dL} + \frac{Q}{R}(2R + Q_\theta)\frac{dR}{dL} \qquad (C2)$$

But

$$Q_\theta = Q\frac{Rd\theta}{dL}$$

so that equation (C2) becomes

$$\left(\frac{g}{\omega^2 r_T}\right)F_\theta = \frac{2Q}{R}(R + Q_\theta)\frac{dR}{dL} + Q^2R\left(\frac{1}{Q}\frac{dQ}{dL}\frac{d\theta}{dL} + \frac{d^2\theta}{dL^2}\right) \qquad (C3)$$

The first term of equation (C3) represents the body force due to radial displacement of the flow (Coriolis force) and the last term represents the force due to tangential acceleration of the fluid resulting from a guiding action by the blades.

REFERENCES

1. Stanitz, John D.: Two-Dimensional Compressible Flow in Turbomachines with Conic Flow Surfaces. NACA Rep. 935, 1949.

2. Stanitz, John D.: Two-Dimensional Compressible Flow in Conical Mixed-Flow Compressors. NACA TN 1744, 1948.

3. Concordia, C., and Carter, G. K.: D-C Network-Analyzer Determination of Fluid-Flow Pattern in a Centrifugal Impeller. Jour. Appl. Mech., vol. 14, no. 2, June 1947, pp. A113-A118.

4. Stanitz, John D., and Ellis, Gaylord O.: Two-Dimensional Compressible Flow in Centrifugal Compressors with Straight Blades. NACA Rep. 954, 1950. (Formerly NACA TN 1932).

5. Ellis, Gaylord O., and Stanitz, John D.: Two-Dimensional Compressible Flow in Centrifugal Compressors with Logarithmic-Spiral Blades. NACA TN 2255, 1950.

6. Wu, Chung-Hua: General Through-Flow Theory of Fluid Flow with Subsonic or Supersonic Velocity in Turbomachines of Arbitrary Hub and Casing Shapes. NACA TN 2302, 1951.

7. Hamrick, Joseph T., Ginsburg, Ambrose, and Osborn, Walter M.: Method of Analysis for Compressible Flow Through Mixed-Flow Centrifugal Impellers of Arbitrary Design. NACA TN 2165, 1950.

8. Ruden, P.: Investigation of Single Stage Axial Fans. NACA TM 1062, 1944.

9. Southwell, R. V.: Relaxation Methods in Theoretical Physics. Clarendon Press (Oxford), 1946.

10. Emmons, Howard W.: The Numerical Solution of Compressible Fluid Flow Problems. NACA TN 932, 1944.

11. Lamb, Horace: Hydrodynamics. Dover Pub., 6th ed., 1945, p. 126.

12. Stodola, A.: Steam and Gas Turbines. Vol. II. McGraw-Hill Book Co., Inc., 6th ed., 1927, p. 991.

13. Milne-Thomson, L. M.: Theoretical Aerodynamics. D. Van Nostrand Co., Inc., 1947, p. 234.

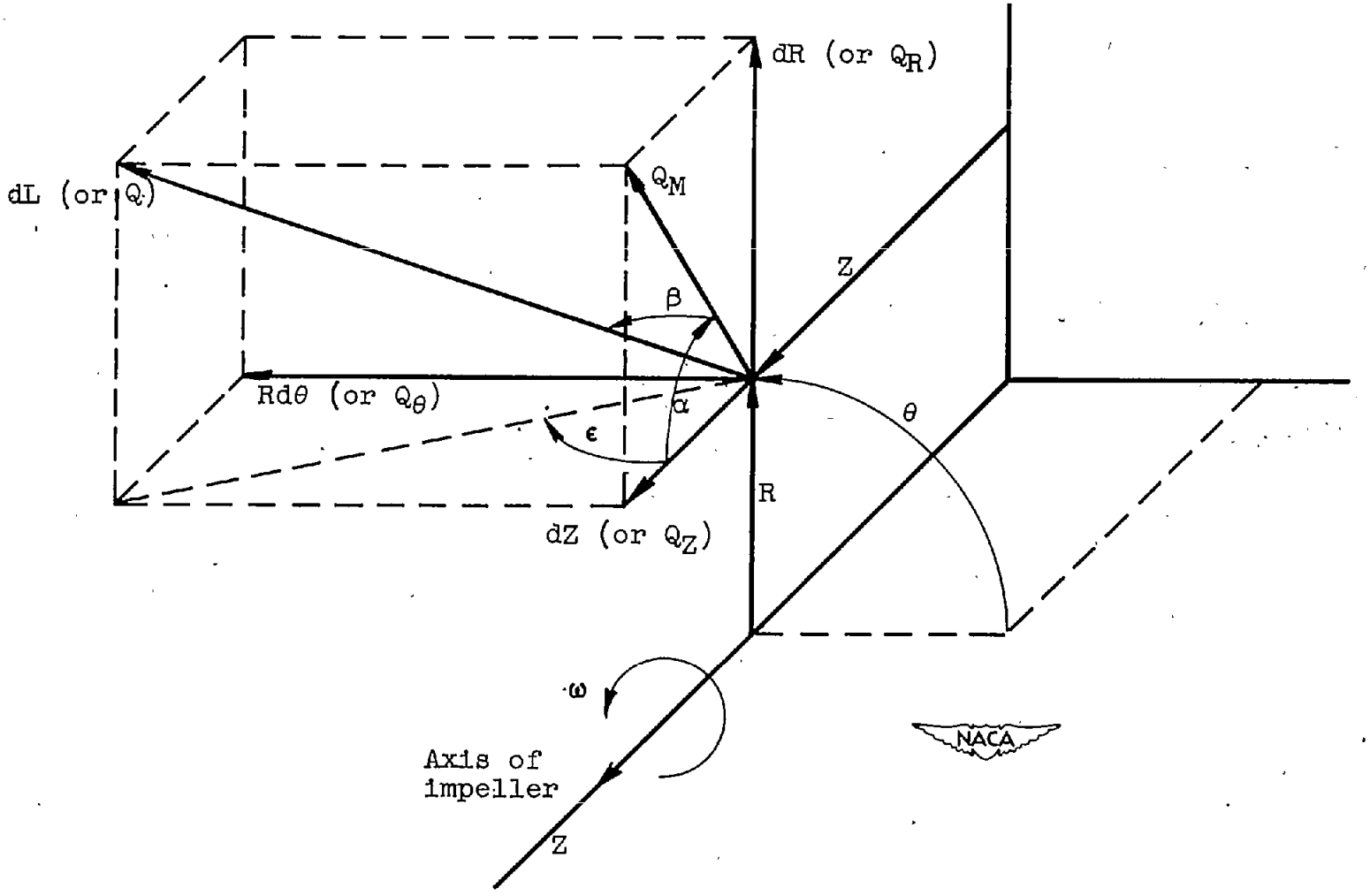

Figure 1. - Cylindrical coordinates (or velocity components) relative to rotating impeller. All quantities dimensionless. Linear coordinates measured in units of impeller tip radius; velocity components measured in units of impeller tip speed.

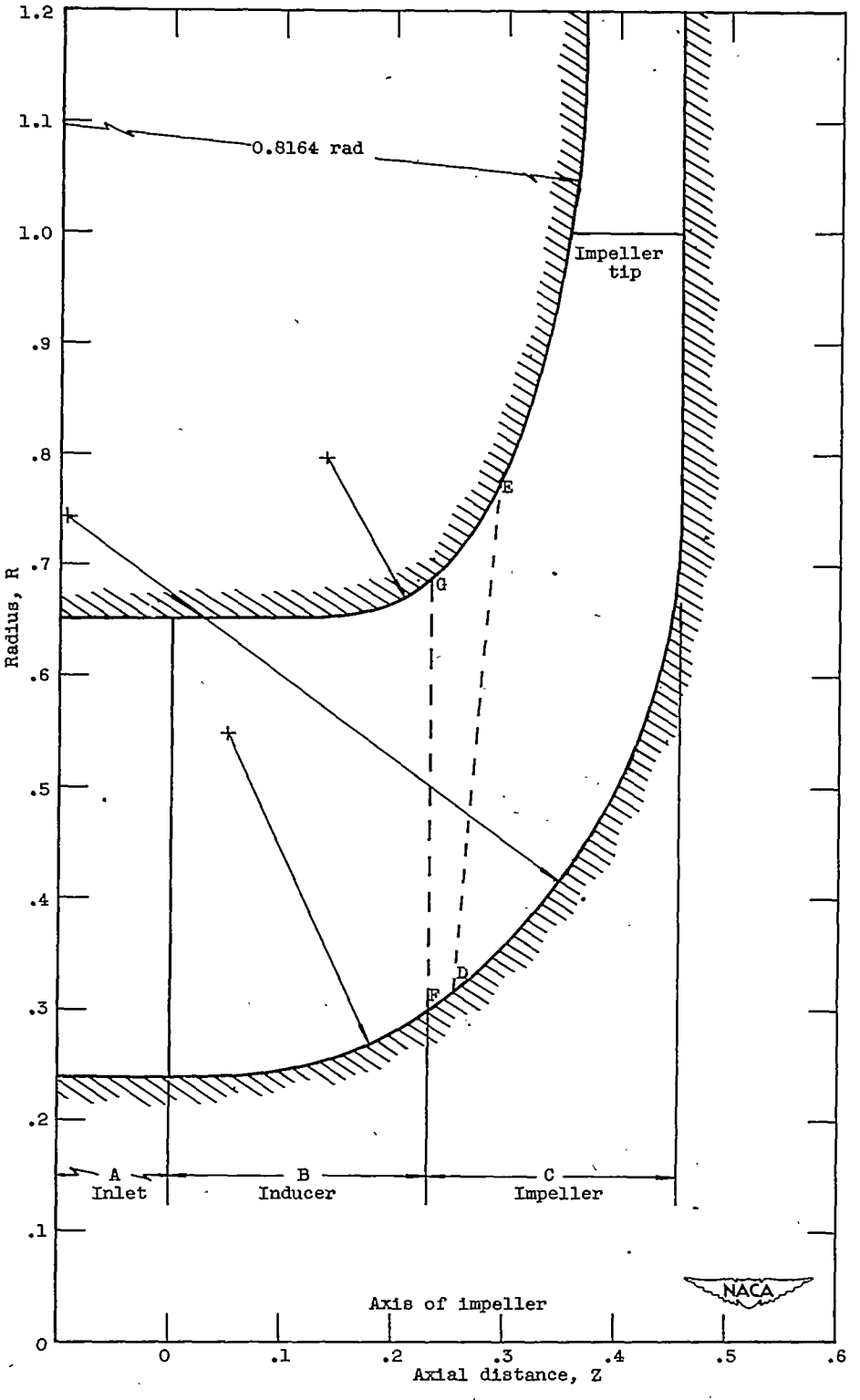

Figure 2. - Hub and shroud dimensions of compressor (divided by tip radius) for axial-symmetry examples I and II. Zero impeller blade thickness; vaneless diffuser.

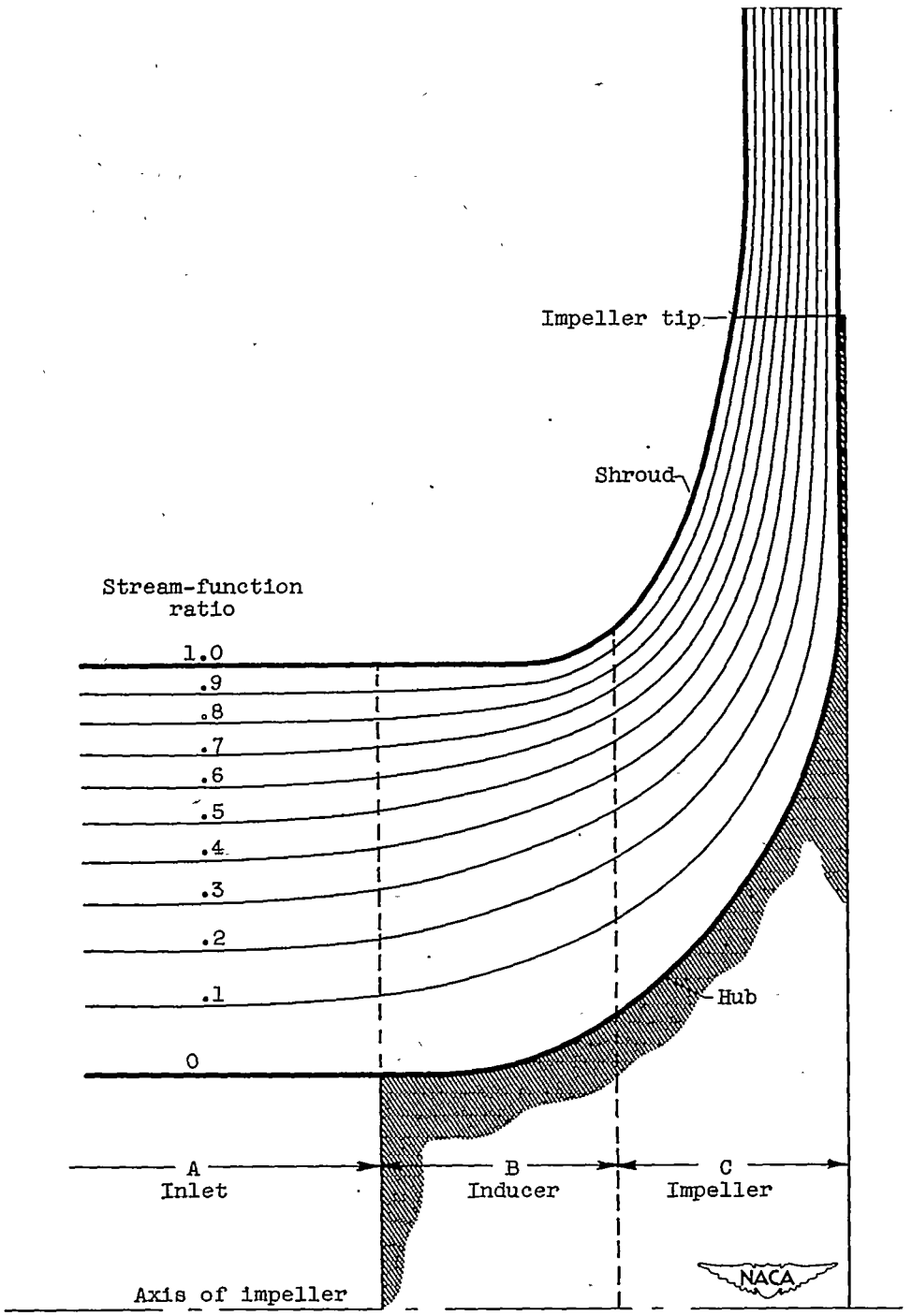

(a) Example IA; impeller with inducer vanes (force field assumed acting upstream of inducer inlet).

Figure 3. - Streamlines in meridional plane for axial-symmetry solution of example I. Streamline designation indicates percentage of flow through compressor between streamline and impeller hub. Incompressible flow; Q_Z equal to 0.3429 far upstream of impeller.

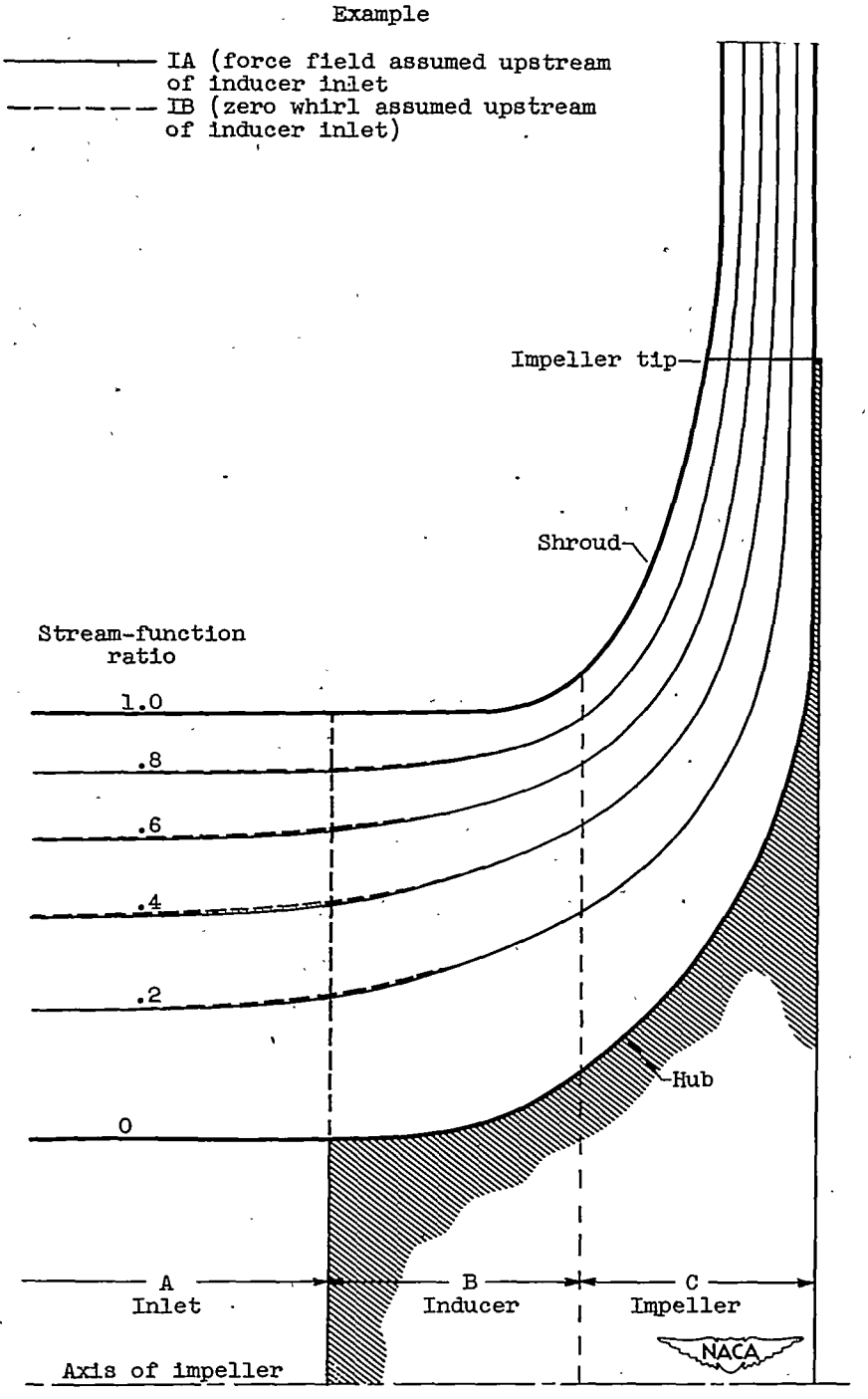

(b) Example IB compared with example IA; impeller with inducer vanes.

Figure 3. - Concluded. Streamlines in meridional plane for axial-symmetry solution of example I. Streamline designation indicates percentage of flow through compressor between streamline and impeller hub. Incompressible flow; Q_Z equal to 0.3429 far upstream of impeller.

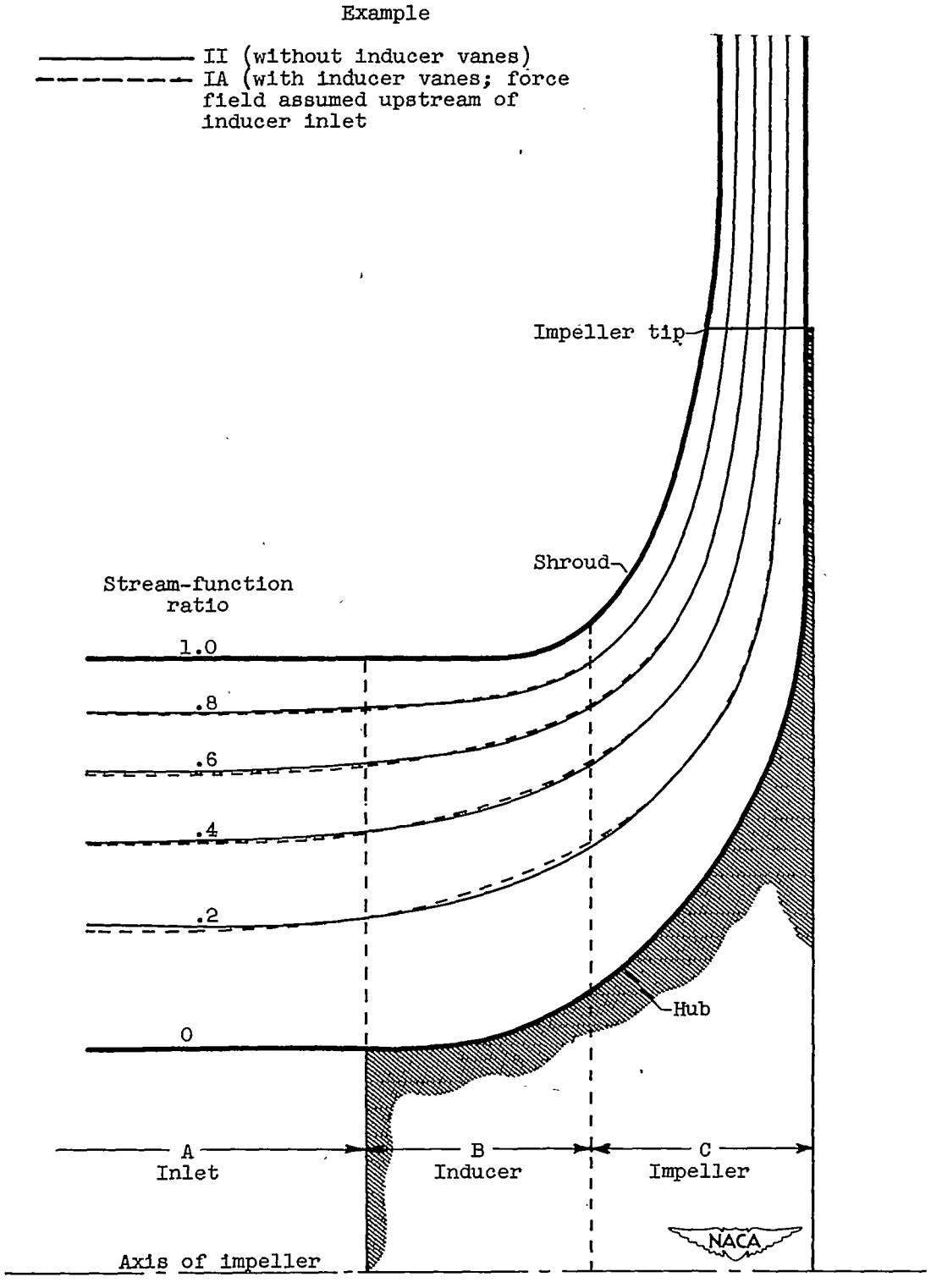

Figure 4. - Comparison of streamlines in meridional plane for axial-symmetry solutions of examples IA and II. Streamline designation indicates percentage of flow through compressor between streamline and impeller hub. Incompressible flow; Q_Z equal to 0.3429 far upstream of impeller.

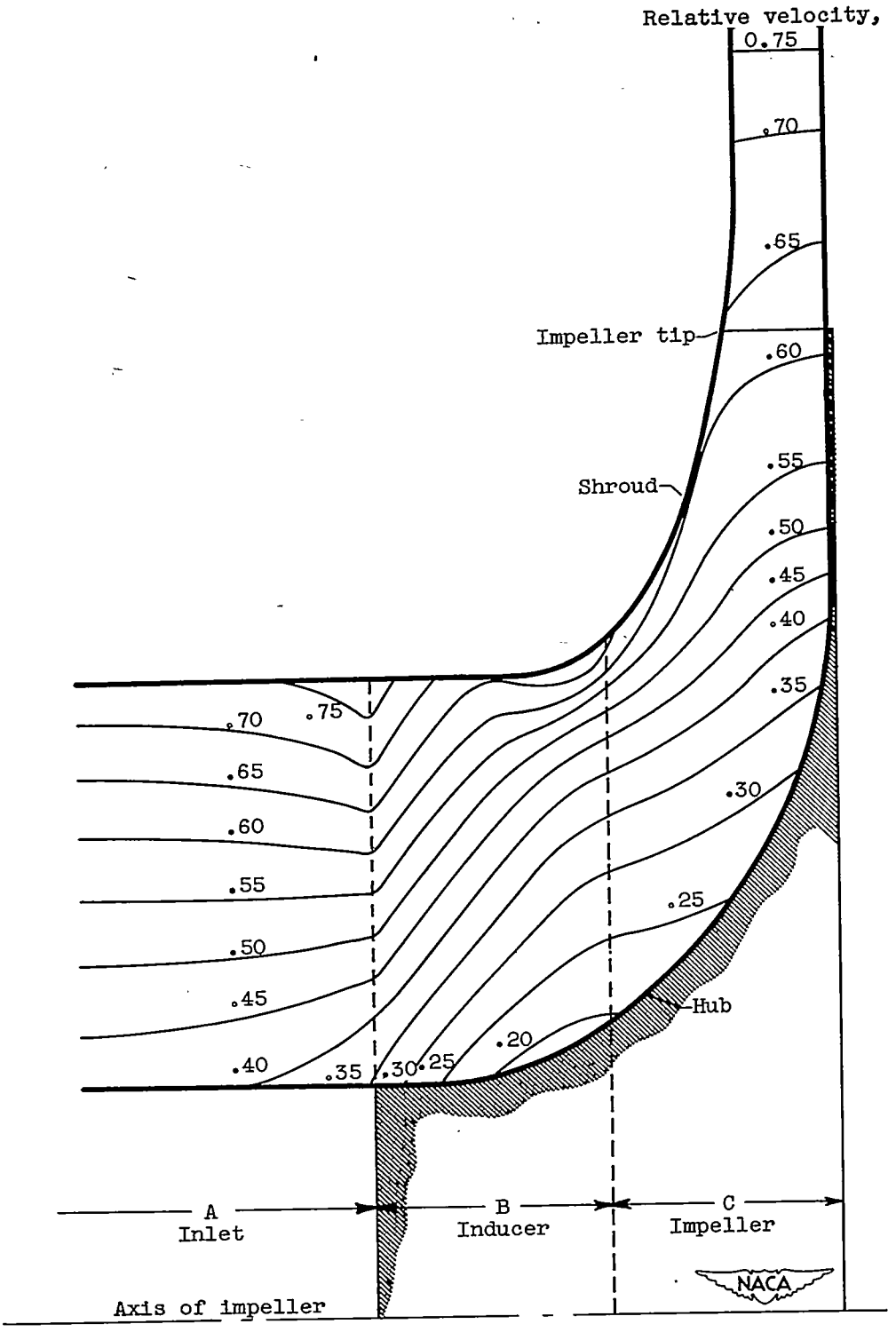

(a) Example IA; impeller with inducer vanes (force field assumed upstream of inducer inlet).

Figure 5. - Lines of constant relative velocity in meridional plane for axial-symmetry solution of example I. Incompressible flow; Q_Z equal to 0.3429 far upstream of impeller.

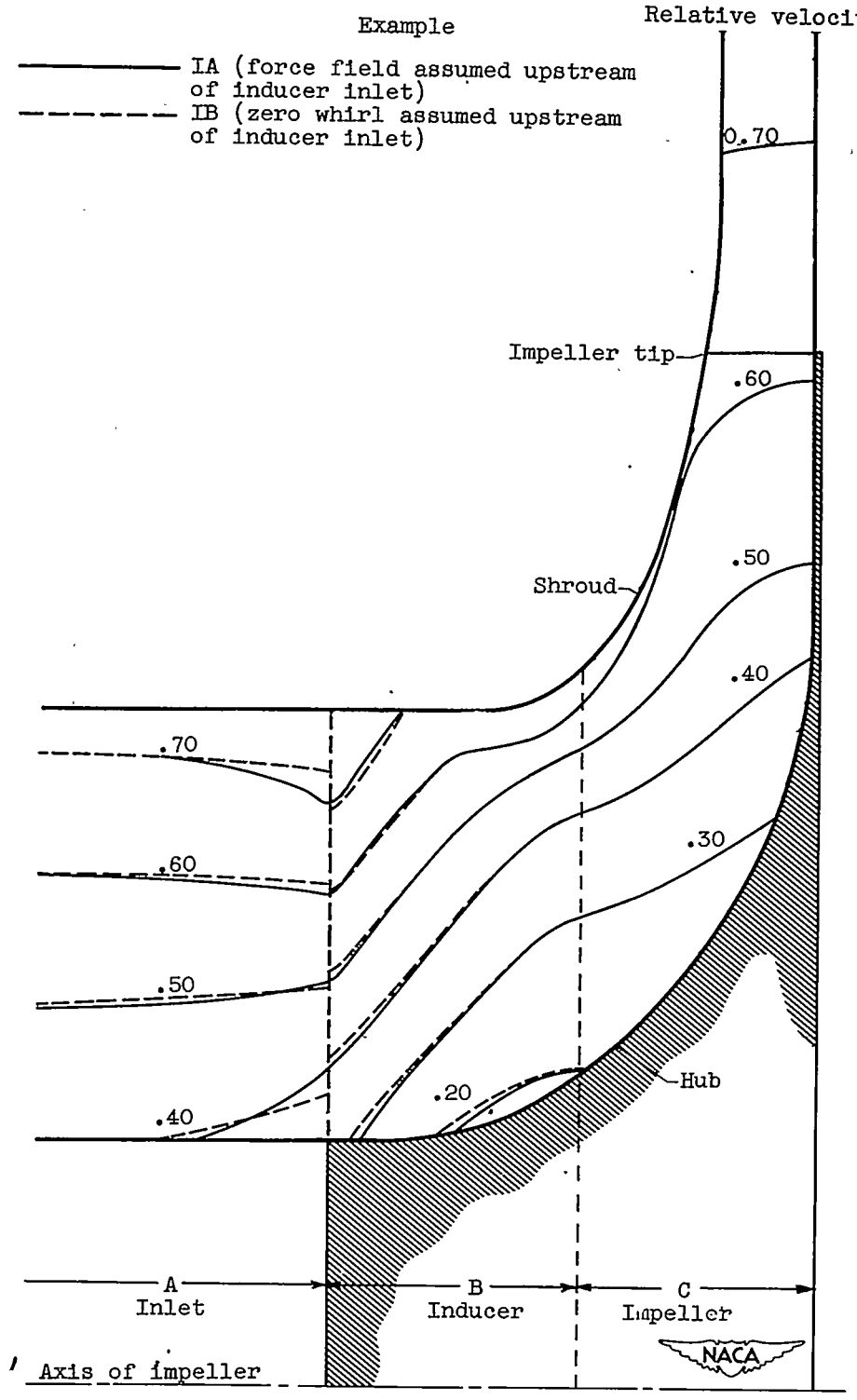

(b) Example IB compared with example IA; impeller with inducer vanes.

Figure 5. - Concluded. Lines of constant relative velocity in meridional plane for axial-symmetry solution of example I. Incompressible flow; Q_Z equal to 0.3429 far upstream of impeller.

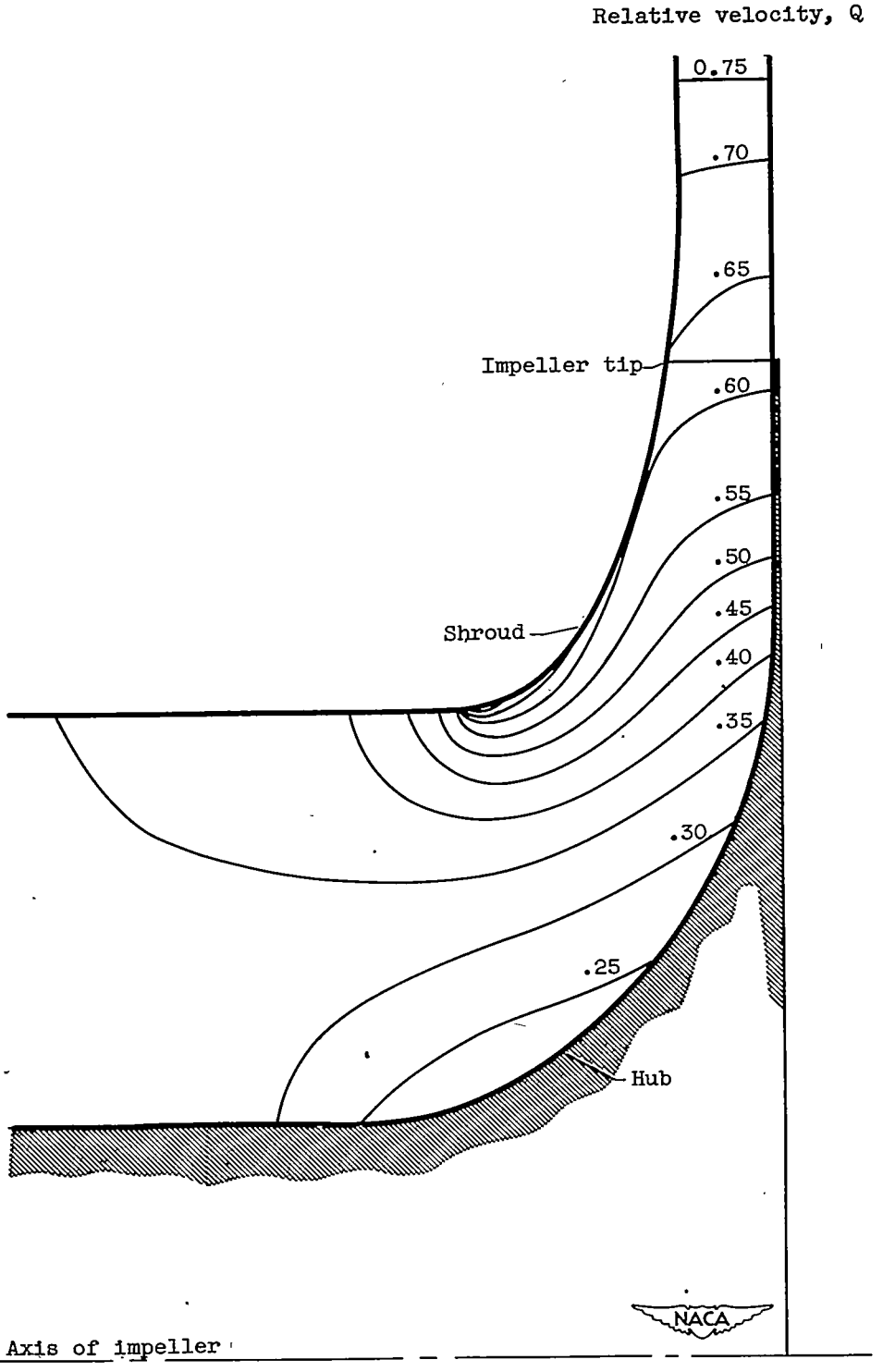

Figure 6. - Lines of constant relative velocity in meridional plane for axial-symmetry solution of example II. Impeller with inducer vanes removed and straight impeller blades extended upstream parallel to axis of compressor. Incompressible flow; Q_Z equal to 0.3429 far upstream of impeller.

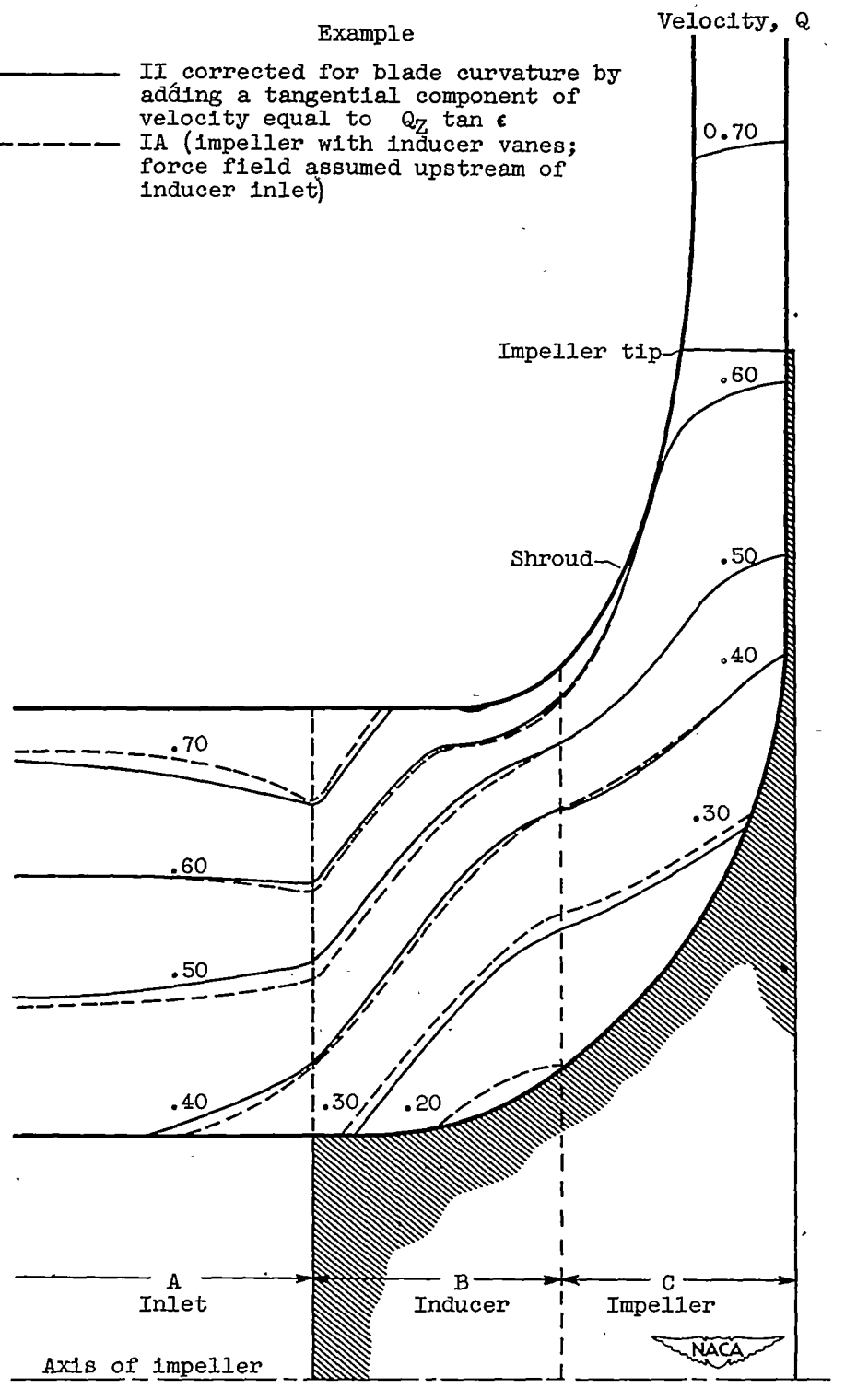

Figure 7. - Relative velocities in impeller without blade curvature corrected for impeller having blade curvature. Incompressible flow; Q_Z equal to 0.3429 far upstream of impeller.

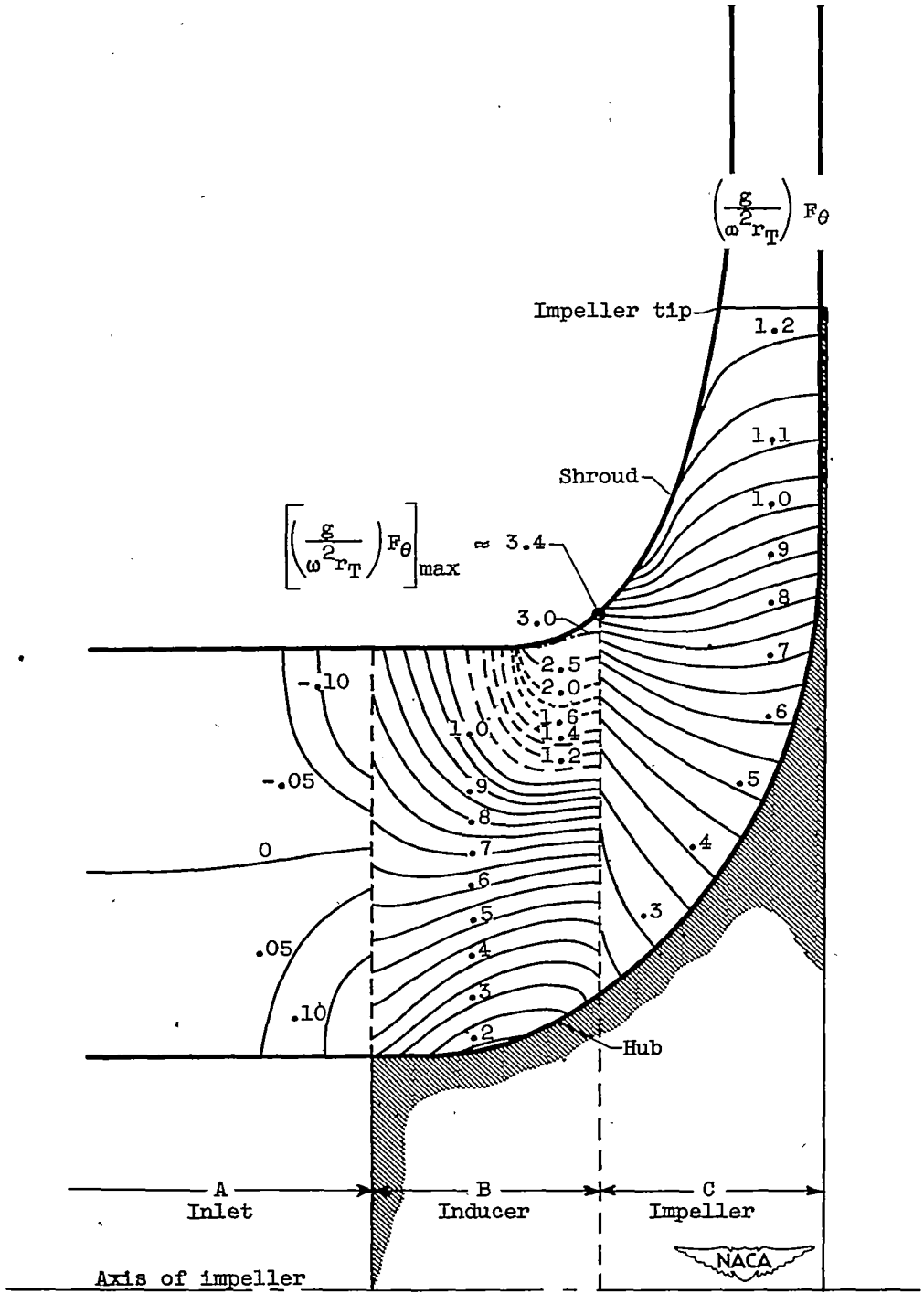

(a) Example IA; impeller with inducer vanes (force field assumed upstream of inducer inlet).

Figure 8. - Tangential component of distributed blade force $(g/\omega^2 r_T)F_\theta$ for axial-symmetry solution of example I. Incompressible flow; Q_Z equal to 0.3429 far upstream of impeller.

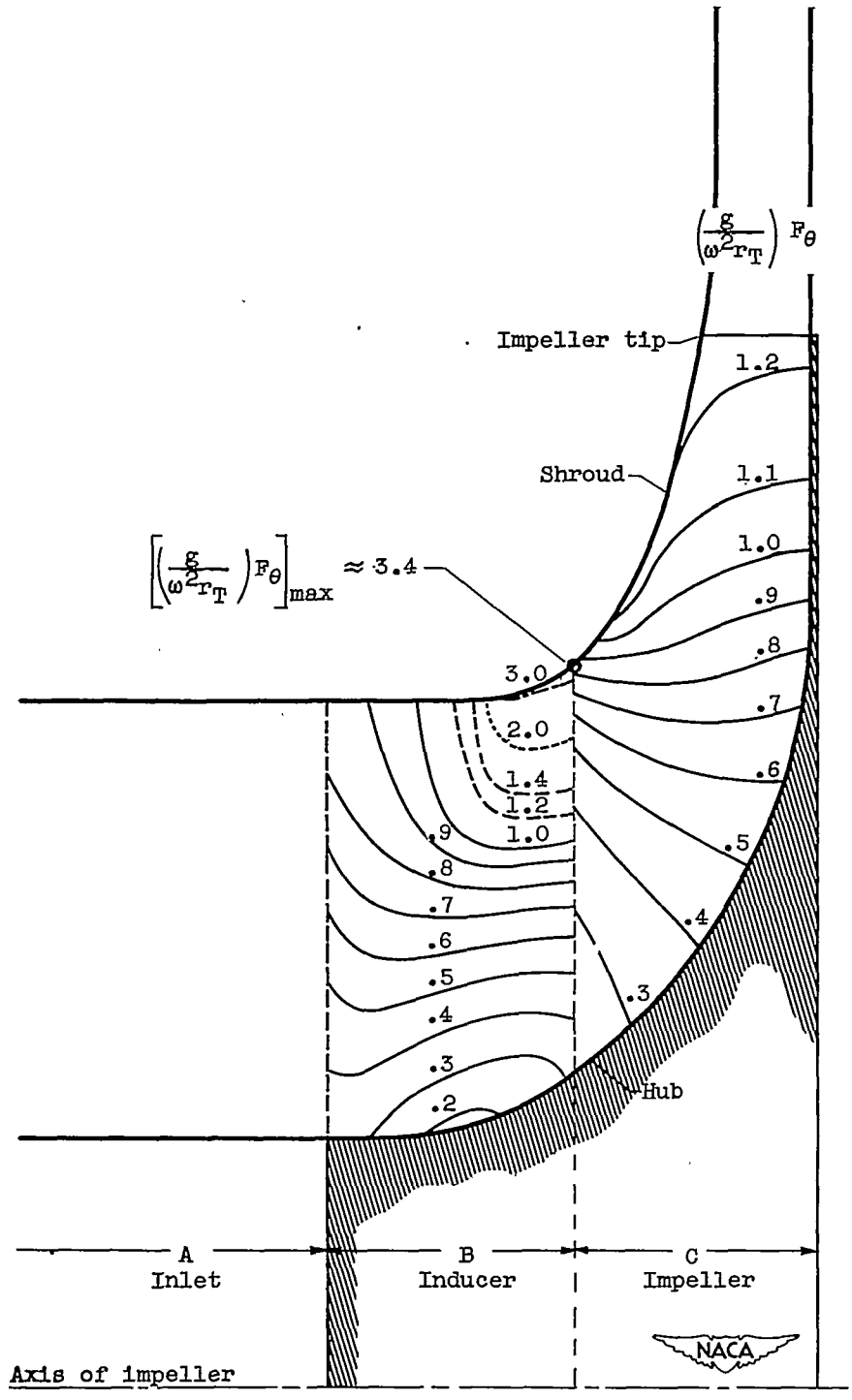

(b) Example IB; impeller with inducer vanes (zero whirl assumed upstream of inducer inlet).

Figure 8. - Concluded. Tangential component of distributed blade force $(g/\omega^2 r_T)F_\theta$ for axial-symmetry solution of example I. Incompressible flow; Q_Z equal to 0.3429 far upstream of impeller.

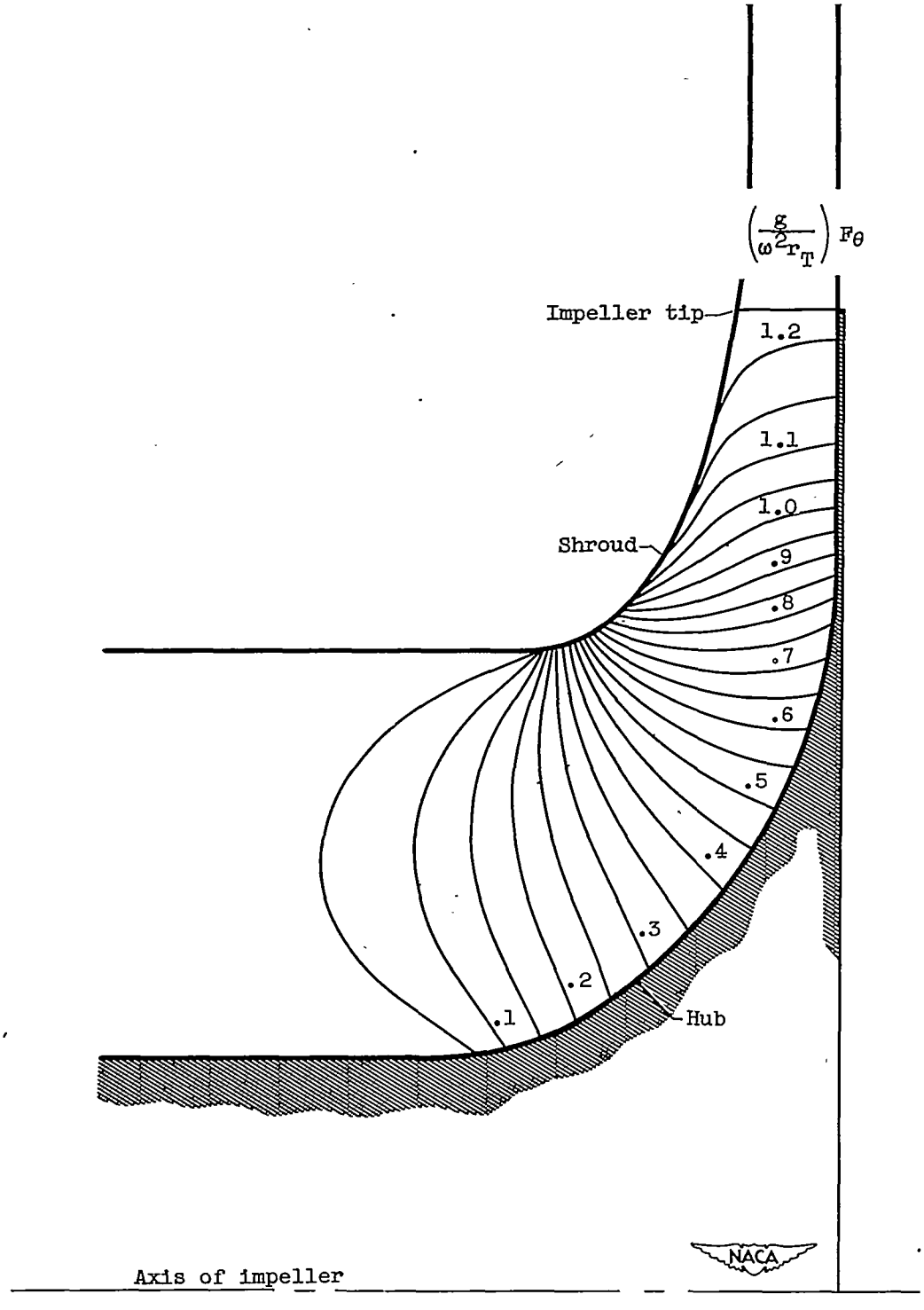

Figure 9. - Tangential component of distributed blade force $(g/\omega^2 r_T)F_\theta$ for axial-symmetry solution of example II. Impeller with inducer vanes removed and straight impeller blades extended upstream parallel to axis of compressor. Incompressible flow; Q_Z equal to 0.3429 far upstream of impeller.

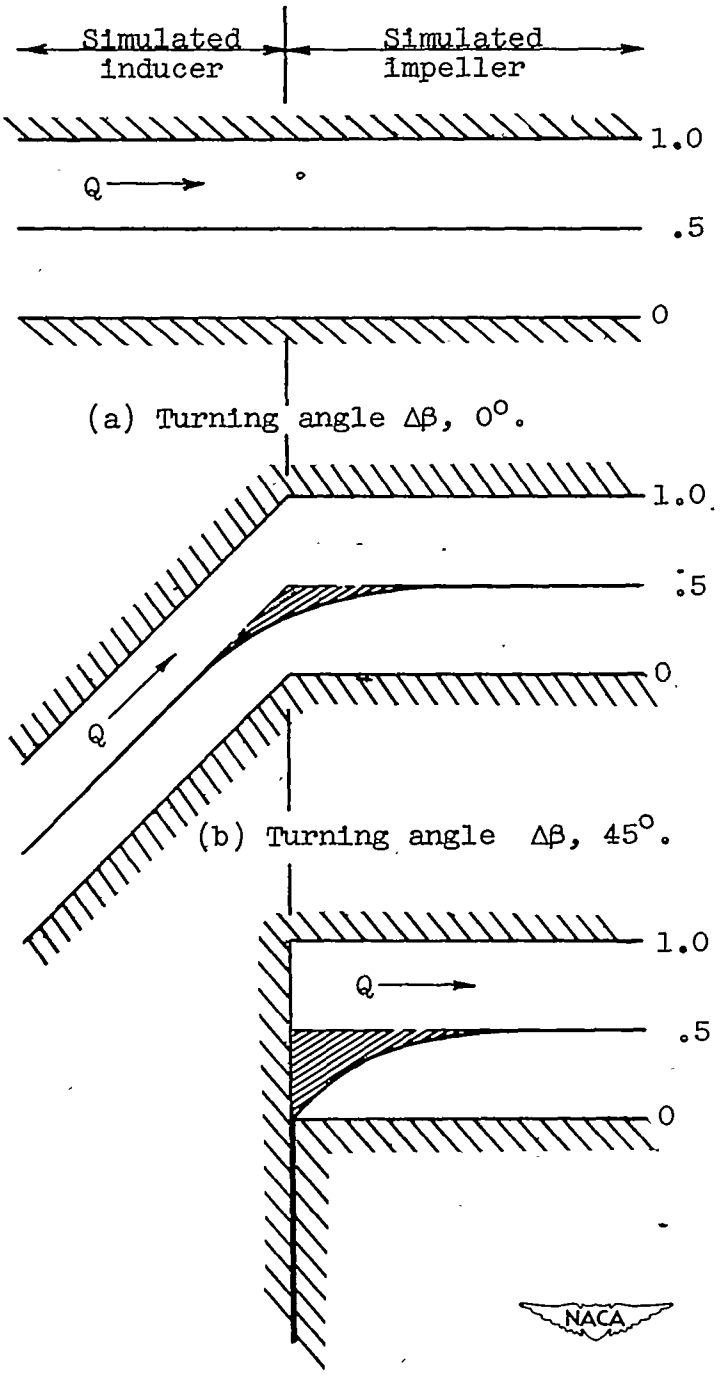

Figure 10. - Incompressible flow between blades of three inducers. Range of turning angle, 0° to 90° with infinite rates of turning. Shaded areas indicate deviation of mean streamline shape from mean blade surface shape.

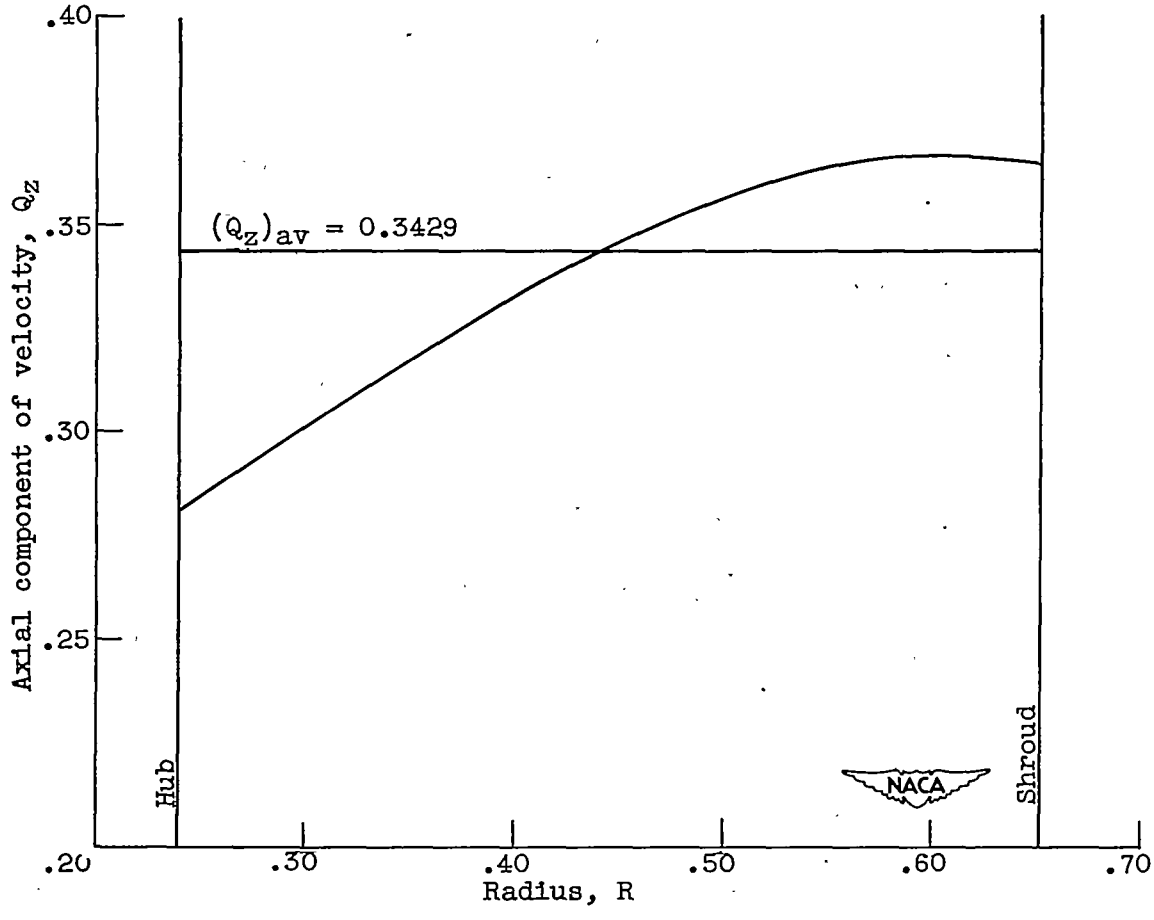

Figure 11. - Variation in axial component of velocity between hub and shroud at inlet for example IA.

NACA-Langley - 9-13-51 - 1000